ELSEVIER

Materials Science and Engineering A 438–440 (2006) 504–508

MATERIALS SCIENCE & ENGINEERING A

www.elsevier.com/locate/msea

Electrochemical corrosion behaviour of $Ti_{44}Ni_{47}Nb_9$ alloy in simulated body fluids

C. Li [a,b], Y.F. Zheng [a,b,*], L.C. Zhao [a]

[a] *School of Materials Science and Engineering, Harbin Institute of Technology, Harbin 150001, China*
[b] *Department of Mechanics and Engineering Science, Peking University, Beijing 100871, China*

Received 15 April 2005; received in revised form 26 December 2005; accepted 28 February 2006

Abstract

The anti-corrosion properties of $Ti_{44}Ni_{47}Nb_9$ shape memory alloy in simulated body fluids including 0.9% NaCl, Hank's and artificial saliva solutions at pH 2.4, 5.4 and 7.4 are investigated by electrochemical measurements. X-ray photoelectron spectroscopy (XPS) is used to characterize the composition and in-depth distribution of the passive films on the alloy as well as their compositional changes before and after linear polarization measurement with the aim to reveal the corrosion mechanism of the $Ti_{44}Ni_{47}Nb_9$ alloy. The open circuit potential (OCP) increases after adding Nb to TiNi alloy. In 0.9% NaCl solutions, the OCP decreases with increasing pH value and it is contrary for artificial saliva solution. Linear polarization results show that pH values and corrosion solutions have different effect on corrosion behaviour of $Ti_{44}Ni_{47}Nb_9$ alloy. The XPS results verify that after linear polarization the passive film forms on the surface of $Ti_{44}Ni_{47}Nb_9$ consisting of TiO_2 and Nb_2O_5. The experimental results prove that the electrochemical corrosion behaviour of TiNi alloy is improved after adding Nb. This implies that $Ti_{44}Ni_{47}Nb_9$ alloy may be used as a promising implant material.

Keywords: $Ti_{44}Ni_{47}Nb_9$ alloy; Electrochemical corrosion; Shape memory alloys; Biomedical materials

1. Introduction

Surface properties and anti-corrosion characteristics are the most important material characteristics determining the biofunctionality of all implant biomaterials. TiNi alloy has been a valuable biomaterial for manufacturing implants due to its unique properties, such as shape memory effect, superelasticity and good mechanical property [1–4]. Many devices, such as stent, orthodontic wires, root canal files, etc., have been used clinically [2,5].

Some studies of the in vitro and in vivo biological properties of TiNi alloy have been reported. It has been found that TiNi alloys have poor local corrosion resistance especially in chloride-containing corrosive media [6]. The toxicity and carcinogenesis of Ni^{2+} ions released from TiNi alloy implant because of corrosion to body become a major concern of this alloy for biological applications [7].

In recent years, ternary TiNi–X alloys have been investigated in hope of improving properties of TiNi alloy as an implant material. Ma and Wu [8] have found that the addition of Ta enhances the corrosion resistance in SBF, and decreases the Ni^{2+} ions release rate in a corrosive environment. Wen et al. [9] also found that the corrosion resistance of $Ti_{50-X}Ni_{50}Cu_X$ ($X = 1$, 2, 4, 6, 8) alloys are better than that of binary TiNi alloys. It is well known that Nb, Zr and Ta exhibit excellent biocompatibility and are non-toxic in tissue interaction. It has been demonstrated that Nb, Zr and Ta are appropriate alloying elements due to their passive oxide layers which possess extremely low solubility and high protective ability.

In the present work, the influence of Nb on the corrosion property of TiNi alloy has been investigated by electrochemical methods.

2. Experimental method

2.1. Sample preparation

The $Ti_{44}Ni_{47}Nb_9$ (numbers indicate at.%) alloy samples were wire cut into 13 mm × 13 mm × 1 mm from a rod prepared by

* Corresponding author. Tel.: +86 10 6276 7760; fax: +86 10 6276 7760.
E-mail address: yfzheng@pku.edu.cn (Y.F. Zheng).

0921-5093/$ – see front matter © 2006 Elsevier B.V. All rights reserved.
doi:10.1016/j.msea.2006.02.185

Table 1
Compositions of test solutions

Components (g/L)	0.9% NaCl	Hank's	Artificial saliva
NaCl	9.00	8.00	0.7
KCl		0.40	1.2
$NaHCO_3$		0.35	1.5
NaH_2PO_4		0.10	
$MgSO_4{\cdot}7H_2O$		0.06	
$Na_2HPO_4{\cdot}2H_2O$		0.12	0.36
$MgCl_2{\cdot}H_2O$		1.00	
Glucose		1.00	
KSCN			0.33
KH_2PO_4			0.2

Table 2
Corrosion potential (mV/SCE) of samples in SBFs with different pH values

Corrosion media	pH value	E_{corr} (mV/SCE)	
		TiNiNb	TiNi
0.9% NaCl solution	2.4	−150	−100
	5.4	−110	−296
	7.4	−50	−140
Hank's solution	2.4	−199	−160
	5.4	−200	−320
	7.4	−60	−360
Artificial saliva solution	2.4	0	−160
	5.4	−160	−380
	7.4	−220	−290

arc-melting method under an Ar atmosphere. The working surfaces of the samples were polished by mechanical method to a mirror finish, and then the samples were cleaned ultrasonically in acetone, ethyl alcohol and distilled water for about 10 min in sequence.

2.2. Electrochemical tests

Open circuit potential (OCP) measurement was conducted by a electrochemical working station (CHI650B, CHN), and Linear Polarization (LP) measurement was performed using a potentiostat/galvanostat (Model 283, PAR/EG&G USA). A platinum and a saturated calomel electrode (SCE) is used as the counter and the reference electrode, respectively. All measurements were tested in simulated body fluids, namely 0.9% NaCl solution, Hank's solution and artificial saliva solution at $(37 \pm 0.5)^\circ$C. Table 1 shows the compositions of test solutions. OCP measurement was maintained up to 24 h and the linear polarization measurement was performed at potentials from −500 to 1300 mV versus SCE in the anodic direction. The scan rate was 60 mV/min. All samples were immersed into electrolyte for 30 min before polarization measurements.

2.3. Characterization of passive films

The composition of the passive films was characterized using an ESCA PHI 500 spectrometer with a Al Kα X-ray source. Ion sputter profiling was performed with a 1 keV Ar^+ ion beam over a 5 mm × 5 mm area at an angle of 50° with respect to the surface.

3. Results and discussion

3.1. Electrochemical behaviour

Table 2 shows the OCP values of $Ti_{44}Ni_{47}Nb_9$ alloy obtained in SBFs at pH 2.4, 5.4 and 7.4. As the table shows, the OCP of the TiNiNb alloy is significantly higher than that of the TiNi alloy in Hank's and artificial saliva solutions. However, in the 0.9% NaCl solutions, the OCP of the TiNiNb alloy is lower than that of TiNi alloy.

Fig. 1 shows the OCP versus immersion time curves of $Ti_{44}Ni_{47}Nb_9$ alloy in 0.9% NaCl solutions at pH 2.4, 5.4 and 7.4. The OCP increase quickly at the beginning of immersion in the pH 7.4 solution, which suggests a protective passive film was formed on the surface of $Ti_{44}Ni_{47}Nb_9$ alloy, and then stabilized at −50 mV/SCE. At pH 5.4, the OCP in corrosion solution decreases sharply at the initial stage then stabilized at −110 mV/SCE. The OCP decreases continuously at pH 2.4 during the whole test, which shows the dissolution of the air-formed passive layer.

Fig. 2(a and b) presents the OCP versus immersion time curves of $Ti_{44}Ni_{47}Nb_9$ alloy in Hank's and artificial saliva solutions at pH 2.4, 5.4 and 7.4, respectively. The OCP in Hank's solutions stabilized at −199, −200 and −60 mV/SCE for the three pH values, respectively. It was observed the OCP fluctuates during immersion in Hank's solution at pH 5.4. In artificial saliva solutions shown in Fig. 2(b), the OCP reaches 0, −160 and −220 mV/SCE after 24 h of immersion for the three pH values, respectively. The tendency is contrary to those in the other two solutions.

Fig. 3 shows the linear polarization diagrams for the $Ti_{44}Ni_{47}Nb_9$ alloy samples in the three SBFs at pH 2.4. As the diagrams show, $Ti_{44}Ni_{47}Nb_9$ alloy demonstrates partial passivating during measurement in Hank's solution, in which case the corrosion current increases slowly with the increasing of potential. In the 0.9% NaCl solution, $Ti_{44}Ni_{47}Nb_9$ alloy exhibits an

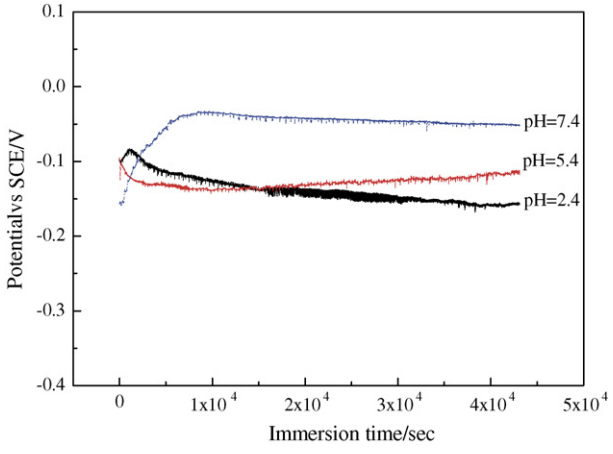

Fig. 1. The OCP vs. immersion time diagrams of $Ti_{44}Ni_{47}Nb_9$alloy in 0.9% NaCl solutions at pH 2.4, 5.4 and 7.4.

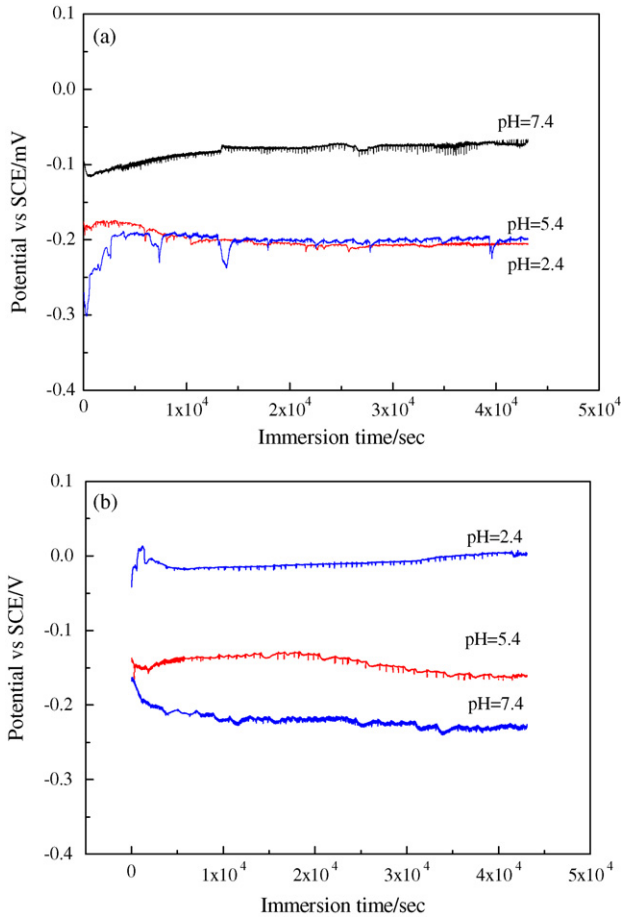

Fig. 2. The OCP vs. immersion time diagrams of $Ti_{44}Ni_{47}Nb_9$ alloy in Hank's and artificial saliva solutions at pH 2.4, 5.4 and 7.4 (a) Hank's solutions and (b) Artificial saliva solutions.

active-to-passive behaviour, and then remains in the passivity state with increasing of potential. In addition, the linear polarization diagram of $Ti_{44}Ni_{47}Nb_9$ alloy obtained in artificial saliva solution has the lowest corrosion current at potentials from E_{corr} to 600 mV/SCE, and then keeps the low corrosion current I_{pass},

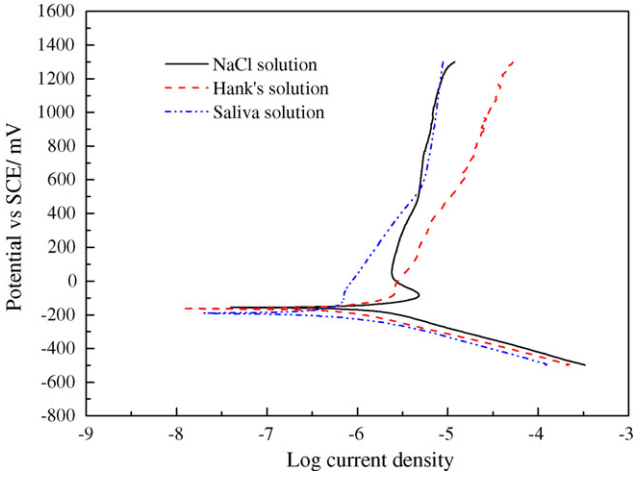

Fig. 3. Representative linear polarization diagrams of $Ti_{44}Ni_{47}Nb_9$ alloy in different SBFs at pH 2.4.

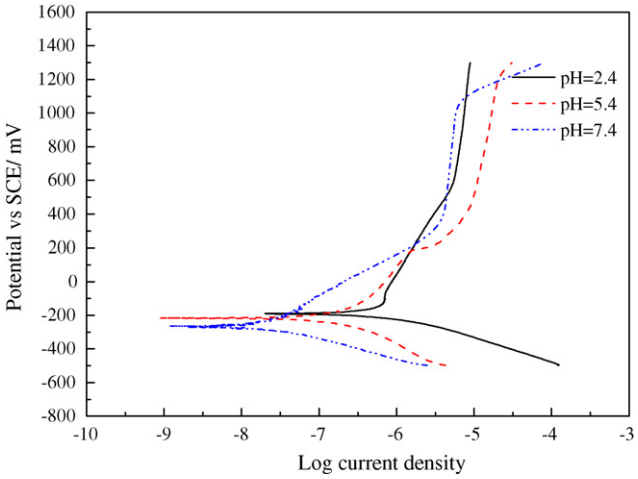

Fig. 4. Representative linear polarization diagrams of $Ti_{44}Ni_{47}Nb_9$ alloy in artificial saliva solutions at pH 2.4, 5.4 and 7.4.

Table 3
The surface atomic percentage of all constitute element in $Ti_{44}Ni_{47}Nb_9$ alloy samples after 3 and 25 min sputtering

Corrosion media	Sputtering time (min)	Element concentration (%)			
		Ni 2p	Ti 2p	O 1s	Nb 3d
Before measurement	3	10.60	27.38	57.43	4.59
	25	51.67	28.17	11.30	8.85
0.9% NaCl solution	3	6.63	28.42	61.03	3.92
	25	58.77	20.21	14.29	6.73
Hank's solution	3	13.32	21.81	61.08	3.79
	25	66.94	17.11	9.56	6.39
Artificial saliva solution	3	14.97	25.48	55.99	3.57
	25	53.71	24.41	15.13	6.75

which is identical to the value in 0.9% NaCl solution and higher than that in Hank's solution.

Fig. 4 presents the linear polarization diagrams of $Ti_{44}Ni_{47}Nb_9$ alloy in artificial saliva solution at pH 2.4, 5.4 and

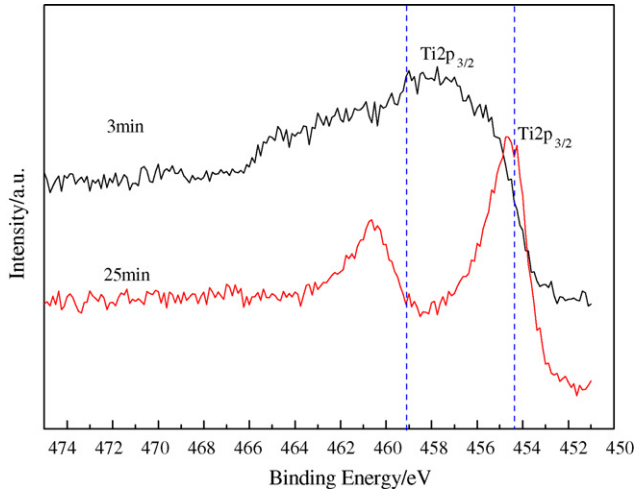

Fig. 5. Ti 2p XPS spectra of $Ti_{44}Ni_{47}Nb_9$ alloy before linear polarization after 3 and 5 min sputtering.

7.4. From the diagrams, it can be noticed that $Ti_{44}Ni_{47}Nb_9$ alloy exhibits an active region from E_{corr} to 600, 300, 200 mV at pH 2.4, 5.4 and 7.4. The passivating tendency is followed. The most significant difference among them is that the passive film is broken at 1100 mV/SCE at pH 7.4, which cannot be observed in other two corrosion solutions.

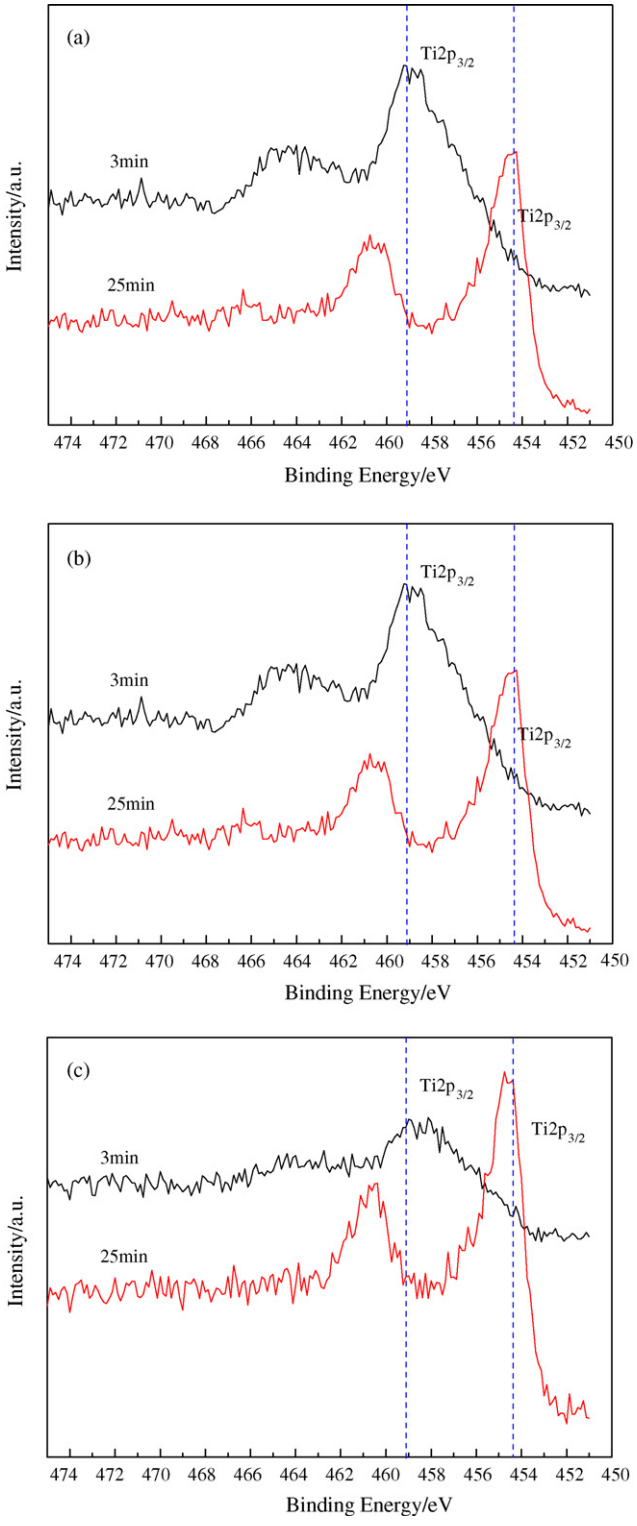

Fig. 6. Ti 2p XPS spectra of $Ti_{44}Ni_{47}Nb_9$ alloy after linear polarization in SBFs at pH 7.4 (a) before corrosion, (b) 0.9% NaCl solution, (c) Hank's solution and (d) artificial saliva solution.

3.2. Surface chemical analysis

Table 3 shows the surface atomic percentage of the constitute element of $Ti_{44}Ni_{47}Nb_9$ alloy samples. The samples were sputtered for 3 and 25 min sputtering before the measurement and after linear polarization test. It is noticeable that the surface after 3 min sputtering consists mainly of O and Ti element for all $Ti_{44}Ni_{47}Nb_9$ alloy samples. After 25 min sputtering, the Ni content increases and the O content decreases significantly comparing with that of 3 min sputtering sample. In addition, Nb content in 25 min sputtering sample is about two times than that in 3 min sputtering sample.

Surface chemical construction of $Ti_{44}Ni_{47}Nb_9$ alloy samples after electrochemical measurement in SBFs at pH 7.4 was analysed using XPS. The Ti 2p, Nb 3d, Ni 2p and O 1s high-resolution spectra indicate that the surface of $Ti_{44}Ni_{47}Nb_9$ alloy samples before linear polarization measurement consists of TiO_2 after 1 min sputtering. However, the Nb 3d spectra obtained after 1 min sputtering show special features of Nb^{5+}, which suggest that the Nb_2O_5 forms during linear polarization measurement besides TiO_2.

Fig. 5 shows the typical Ti 2p high-resolution spectra of $Ti_{44}Ni_{47}Nb_9$ alloy samples before linear polarization measurement. It can be seen that the broad Ti $2p_{3/2}$ peak is insufficient to be indexed as any of the special features of Ti, which suggests the surface of $Ti_{44}Ni_{47}Nb_9$ alloy consists of non-stoichiometric Ti oxide states after 3 min sputtering time. With the sputtering process proceeding, the position of main peak Ti 2p spectra obtained after 25 min sputtering are located at 460 and 454 eV with the characteristic of Ti.

Fig. 6(a–c) presents the typical Ti 2p high-resolution spectra of $Ti_{44}Ni_{47}Nb_9$ alloy samples after linear polarization in SBFs at pH 7.4 with two different sputtering times. As the spectra shows, Ti^{4+} peak increases significantly especially for 0.9% NaCl and Hank's solutions, which confirms that the passive film of $Ti_{44}Ni_{47}Nb_9$ alloy still consist mainly of TiO_2, and the surface after 25 min sputtering is proved to be the $Ti_{44}Ni_{47}Nb_9$ alloy itself. It is similar to the results in Fig. 5.

4. Conclusions

The present work reports the results of electrochemical tests conducted in SBFs at pH 2.4, 5.4 and 7.4. It can be summarized as follows:

(1) The OCP potentials increase in mostly experimental corrosion solutions after adding Nb element to TiNi alloy.
(2) In pH 2.4 SBFs, the linear polarization of $Ti_{44}Ni_{47}Nb_9$ alloy samples in Hank's solution shows partial passivation. The corrosion current obtained in artificial saliva solution is the lowest from E_{corr} to 1100 mV/SCE, then keeps at a low E_{corr} identical to that in 0.9% NaCl solution, which is higher than that obtained in artificial saliva solution.

(3) The outer passive film of $Ti_{44}Ni_{47}Nb_9$ alloy before electrochemical corrosion test consists of a layer of TiO_2, then non-stoichiometric Ti oxide states after 3 min sputtering, after 25 min sputtering it reveals to be the characteristic of metallic Ti. After linear polarization measurement, the oxides of $Ti_{44}Ni_{47}Nb_9$ alloy consist of TiO_2 and Nb_2O_5, only TiO_2 can be found after 3 min sputtering, oxides disappear after 25 min sputtering.
(4) The electrochemical corrosion behaviour of TiNi alloy improved after adding Nb element. It can be concluded that $Ti_{44}Ni_{47}Nb_9$ alloy may be used as a promising implant material.

References

[1] U. Kamachi Mudali, T.M. Sridhar, R.A.J. Baldev, Sadhana 28 (2001) 601.
[2] T.W. Duerig, MRS Bull. 27 (2002) 101.
[3] S.A. Shabalovskaya, Int. Mater. Rev. 46 (2001) 233.
[4] T. Duerig, A. Pelton, D. Stöckel, Mater. Sci. Eng. A 273–275 (1999) 149.
[5] T.W. Duerig, D.E. Tolomeo, M. Wholey, Min. Invas. Ther. Allied. Technol. 9 (2000) 235.
[6] D. Starosvetsky, I. Gotman, Biomaterials 22 (2001) 1853.
[7] M. Berger-Gorbet, B. Broxup, C. Rivard, L.H. Yahia, J. Biomed. Mater. Res. 32 (1996) 243.
[8] J.L. Ma, K. Wu, Proc. SMST (2000) 291.
[9] X. Wen, N. Zhang, X. Li, Z. Gao, Biomed. Mater. Eng. 7 (1997) 1.